

DCE-MRI Data Analysis for Cancer Area Classification

U. Castellani¹; M. Cristani¹; A. Daducci²; P. Farace²; P. Marzola²; V. Murino¹; A. Sbarbati²

¹Department of Computer Science, University of Verona, Verona, Italy;

²Department of Morphological and Biomedical Sciences, Anatomy and Histology Section, University of Verona, Verona, Italy

Keywords

DCE-MRI, cluster analysis, classification, SVM

Summary

Objectives: The paper aims at improving the support of medical researchers in the context of in-vivo cancer imaging. Morphological and functional parameters obtained by dynamic contrast-enhanced MRI (DCE-MRI) techniques are analyzed, which aim at investigating the development of tumor microvessels. The main contribution consists in proposing a machine learning methodology to segment automatically these MRI data, by isolating tumor areas with different meaning, in a histological sense.

Methods: The proposed approach is based on a three-step procedure: i) robust feature extraction from raw time-intensity curves, ii) voxel segmentation, and iii) voxel classification based on a learning-by-example approach. In the first step, few robust features that compactly represent the response of the tissue to the DCE-MRI analysis are computed.

The second step provides a segmentation based on the mean shift (MS) paradigm, which has recently shown to be robust and useful for different and heterogeneous clustering tasks. Finally, in the third step, a support vector machine (SVM) is trained to classify voxels according to the labels obtained by the clustering phase (i.e., each class corresponds to a cluster). Indeed, the SVM is able to classify new unseen subjects with the same kind of tumor.

Results: Experiments on different subjects affected by the same kind of tumor evidence that the extracted regions by both the MS clustering and the SVM classifier exhibit a precise medical meaning, as carefully validated by the medical researchers. Moreover, our approach is more stable and robust than methods based on quantification of DCE-MRI data by means of pharmacokinetic models.

Conclusions: The proposed method allows to analyze the DCE-MRI data more precisely and faster than previous automated or manual approaches.

DCE-MRI techniques represent noninvasive ways to assess tumor vasculature, based on dynamic acquisition of MR images after injection of suitable contrast agents and subsequent voxel-by-voxel quantitative analysis of the signal intensity time curves.

Our method extends our previous work proposed in [3], and brings two advantages to the current state of the DCE-MRI analysis. First, it allows a more stable and robust feature extraction step from DCE-MRI raw data. In fact, as highlighted in [4–6], the standard quantification of DCE-MRI data by means of pharmacokinetic models [7] suffers from large output variability, which is a consequence of the large variety of models employed. Here, we propose to work directly on the raw signals by extracting few and significant features which robustly summarize the time-curve shape of each voxel. Second, we focus on the automation of the whole data-analysis process by exploiting the effectiveness of the machine learning techniques on the proposed applicative scenario. A three-step procedure is introduced: i) signal feature extraction, ii) automatic voxel segmentation, and iii) voxel classification. In the first step, few compact features are computed, without the need of a free parameter tuning procedure. Note that the same features are used for all subjects and for all kinds of tumor. In the second step, the subject voxels are clustered basing on the features previously extracted, by adopting the mean shift clustering [8]. Although the MS clustering approach allows a precise data segmentation, it requires a careful tuning of a free parameter, namely the *bandwidth* [8]. For this reason, we propose to estimate such a parameter on a small subset of the subjects, being supported by the medical researchers that validate the segmentations. Then, in the third step, a classifier is trained to classify the tumoral regions according to the previously validated clustering results. A support vector machine (SVM) [9]

Correspondence to:

U. Castellani
Department of Computer Science
University of Verona
Strada le Grazie 15
37134 Verona
Italy
E-mail: umberto.castellani@univr.it

Methods Inf Med 2009; 48: 248–253

doi: 10.3414/ME9224

prepublished: March 31, 2009

1. Introduction

Machine learning techniques are becoming important to support medical researchers in analyzing biomedical data. For instance, in the context of cancer imaging, methods for the automatic isolation of interest areas characterized by different tumoral tissue development are crucial for diagnosis and therapy assessment [1]. In this paper, morphological

and functional parameters obtained by a dynamic contrast-enhanced MRI (DCE-MRI) acquisition system are analyzed by combining clustering^a and classification techniques [2].

^a In the following, we adopt the terms *segmentation* and *clustering* associating them the same meaning, i.e., the one of a consistent partition of data into classes with high inter-class variance and low intra-class variance [2].

is applied as classifier. In particular, voxels of the same cluster are fed with the same label into the classifier. In this fashion, the SVM becomes able to perform segmentations on new unseen subjects with the same kind of tumor.

In a previous paper [3], we proposed the introduction of the MS clustering on the DCE-MRI data of tumoral regions. In that case, we focused on standard tumor microvessel parameters, such as transendothelial permeability (kPS) and fractional plasma volume (fPV), obtained voxel-by-voxel from intensity time curves. In this paper, we are inspired by recent works on the use of machine learning techniques for DCE-MRI tumor analysis [6, 10–12]. In [6] the curve patterns of the DCE-MRI pixels are analyzed in the context of musculoskeletal tissue classification. Several features are extracted to represent the signal shape such as the maximum signal intensity, the largest positive signal difference between two consecutive scans, and so on. Then, the classification is carried out by introducing a thresholding approach. In [10] the authors proposed the use of the MS algorithm [8] for the clustering of breast DCE-MRI lesions. In particular, pixels are clustered according to the area under the curve feature. Since the results are over-segmented, an iterative procedure is introduced to automatically select the clusters which better represent the tumor. In [11] a learning-by-example approach is introduced to detect suspicious lesions in DCE-MRI data. The tumoral pixels are selected in a supervised fashion and fed to a SVM which is trained to perform a binary classification between healthy and malicious pixels. The raw n -dimensional signal is used as multidimensional vector. In [12] a neural network was applied on dynamic contrast agent MRI sequences as a nonlinear operator in order to enhance differences in the signal courses of pixels of normal and injured tissues.

In this paper we emphasize the use of machine learning techniques as mean to produce stable and meaningful segmentation results in an automatic fashion. Indeed, the proposed approach permits to fasten the analysis itself, ensuring a higher throughput that turns out to be useful in the case of massive analysis.

2. The DCE-MRI Experimental Setup

The main purpose of DCE-MRI analysis is to accurately monitor the local development of cancer, eventually subject to different treatments. Tumor growth is critically dependent on the capacity to stimulate the development of new blood vessels (angiogenesis), which in turn provides the tumor tissue with nutrients. In consequence, various angiogenesis inhibitors have been developed to target vascular endothelial cells and to block tumor angiogenesis [13]. The traditional criteria to assess the tumor response to treatment is based on the local measurement of tumor size change [13]. But such methods of testing cytotoxic compounds might not be adequate for antiangiogenesis drugs, which are in fact mainly cytostatic, slowing or stopping tumor growth. Moreover, the vascular effect of antiangiogenesis drugs may precede, by a remarkably long time interval, the effect on tumor growth. Consequently a different and more appealing indicative symptom of the cancer development has been analyzed, i.e. the tissue vascularization [14]. DCE-MRI techniques play a relevant role in this field [14]. The final aim is to provide quantitative measures that indicate the level of vascularization in the cancer tissue, eventually treated with antiangiogenic compounds, in a *noninvasive* way.

The standard^b DCE-MRI analysis can be divided in the following steps: 1) injecting contrast agents in the subject being analyzed; 2) acquiring MRI image sets of different slices of the tissues of interest; 3) extracting morphological and functional parameters such as *fractional plasma volume* (fPV) and *transendothelial permeability* (kPS), that model the tissue vascularization; in practice, to each point of the MRI image is associated a couple of fPV and kPS values; 4) manually selecting a Region Of Interest on the MRI slices, in order to isolate the highly vascularized local tumoral area; 5) averaging the values of fPV and kPS in such an area, obtaining for each slice a couple of fPV and kPS mean values that indicate the overall level of vasculariza-

tion. Even if the use of fPV and kPS parameters is employed in recent researches [13], such standard tumor microvessel parameters, based on the definition of a particular pharmacokinetic model, suffer from large output instability [4–6].

In this paper, we strongly improve the classical DCE-MRI analysis, providing an automatic method of tumoral tissue classification; the proposed technique is applied to this particular kind of analysis, but we suppose it can also be applied in general in the DCE-MRI context. In detail, we change steps 3, 4 and 5; our method takes as input the raw DCE-MRI signals; in an automatic fashion, it is able to segment areas that correspond to the tumoral area traditionally extracted by hands in step 4, driven by histological and physiological a-priori considerations.

3. Proposed Method

The proposed methodology is based on three main steps: i) signal feature extraction, ii) MS clustering, and iii) SVM classification. In the first step we extract standard curve parameters [6, 10]. The aim is to define a compact representation of the signal curve shape of each voxel, which effectively summarize the expected behavior by medical researchers. In the second step we choose the MS method since it effectively performs a clustering of multidimensional data lying on regular grid (i.e., the image) by combining spatial and feature relations into the same framework [8]. After the previous step, few stable and meaningful regions are extracted. In order to improve the automation of the proposed system, the data (i.e., voxel) segmentation can be treated as a classification problem on which a classifier is trained to distinguish among the regions extracted by the clustering. In particular, the number of regions is fixed according to the expectations of the medical researchers. Therefore, in the third step we select the SVM as classifier. We highlight that SVM are particular suitable for our method since we naturally define a n -dimensional feature vector for each voxel, as required by the SVM framework. Moreover, SVM have already shown their efficacy on several domains, by performing a data-driven classification while being able to effectively generalize the results [2].

^b The procedure listed above comes from the investigation detailed in [13], that in turn presents additional similar researches.

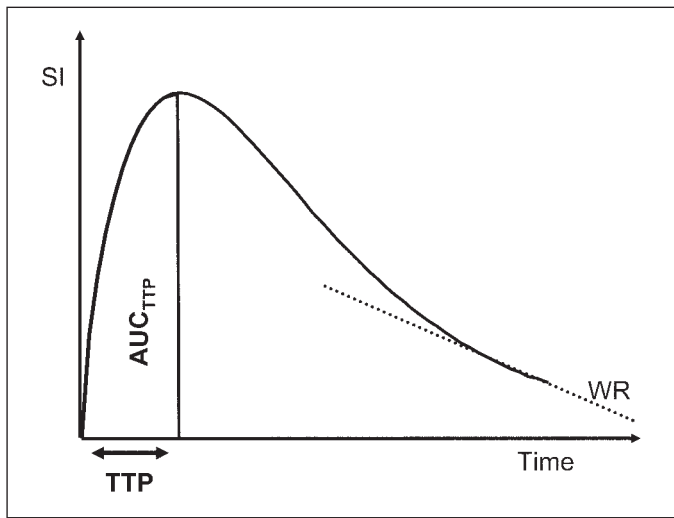


Fig. 1 Signal feature extraction: TTP, AUC, AUC_{TTP}, and WR (see text)

3.1 Signal Feature Extraction

From the raw DCE-MRI signals, few and stable features are extracted. For each voxel, the time-intensity curve is divided by the pre-contrast signal intensity value in order to normalize signal intensities out of the scanner. Furthermore, data is filtered with a smoothing function to minimize errors due to outliers collected during the feature extraction step. More in details, the extracted features are:

- Time to peak (TTP) is the time interval between contrast injection and the time of maximum of signal intensity (SI).
- Area under the curve (AUC) is the integral of the time-intensity curve.
- AUC_{TTP} is the integral of the time-intensity curve between contrast injection and the time of maximal signal intensity.
- Washout rate (WR) is the mean approximate derivative of the last part of the time-intensity curve.

Note that proposed features depend only on the time signal observed on a single voxel being independent by the respective contextual neighborhood. In order to give the same weight to all of these features during the clustering step, a standardization procedure is performed, i.e., the range of each feature is normalized to the unit interval. ▶ Figure 1 shows a scheme of the visual meaning of the extracted features.

3.2 Mean-shift Clustering

The theoretical framework of the Mean Shift (MS) [8] arises from the ParzenWindows technique [2], that, in particular hypotheses of regularity of the input space (such as independency among dimensions [8]), estimates the density at point \mathbf{x} as:

$$\hat{f}_{h,k}(\mathbf{x}) = \frac{c_{k,d}}{nh^d} \sum_{i=1}^n k\left(\left\|\frac{\mathbf{x}-\mathbf{x}_i}{h}\right\|^2\right) \quad (1)$$

where d indicates the dimensionality of the data processed, n is the number of points

$$\nabla \hat{f}_{h,k}(\mathbf{x}) = \frac{2c_{k,d}}{nh^d} \cdot \left[\sum_{i=1}^n g\left(\left\|\frac{\mathbf{x}_i-\mathbf{x}}{h}\right\|^2\right) \right] \cdot \left[\frac{\sum_{i=1}^n \mathbf{x}_i g\left(\left\|\frac{\mathbf{x}_i-\mathbf{x}}{h}\right\|^2\right)}{\sum_{i=1}^n g\left(\left\|\frac{\mathbf{x}_i-\mathbf{x}}{h}\right\|^2\right)} - \mathbf{x} \right]$$

Fig. 2 Equation 2

available, and $k(\cdot)$ is the kernel profile that models how strongly the points are taken into account for the estimation, in dependence with their distance to \mathbf{x} , influenced by the h term. Finally, $c_{k,d}$ is a normalizing constant, depending on the dimensionality of the data and on the kernel profile.

MS extends this “static” expression, differentiating (1) and obtaining the gradient of the density (▶ see Fig. 2), where $g(x) = \frac{\delta k(x)}{\delta x}$.

In Equation 2, the first term in square brackets is proportional to the normalized density gradient, and the second term is the mean shift vector $M_v(x)$, that is guaranteed to point towards the direction of maximum increase in the density [8].

Therefore, the MS vector can define a path leading to a stationary point of estimated density. The modes of the density are such stationary points. More in details, starting from a point \mathbf{x} in the feature space, the mean shift procedure consists in calculating the mean shift vector at \mathbf{x} , which will head to location $\mathbf{y}^{(1)}$; this process is applied once again to $\mathbf{y}^{(1)}$, producing location $\mathbf{y}^{(2)}$ and so on, until a convergence criterion is met, and a convergence location \mathbf{y} is reached. The mean shift procedure is guaranteed of being convergent [8].

In the MS-based clustering, from here simply MS clustering, the first step is made by applying the MS procedure to all the points $\{\mathbf{x}_i\}$, producing the convergency points $\{\mathbf{y}_i\}$. A consistent number of close convergency locations $\{\mathbf{y}_i\}_l$ indicates a mode μ_l . The clustering operation consists in marking the corresponding points $\{\mathbf{x}_i\}_l$ that produces the set $\{\mathbf{y}_i\}_l$ with the label l . This happens for all the convergency locations $l = 1, 2, \dots, L$.

In this clustering framework, the only interventions required by the user involve the choice of the kernel profile $k(\cdot)$ and the choice of bandwidth value h . As usual, the Epanechnikov kernel is adopted as kernel profile [8]. Note that, in this fashion, the meaning of the kernel bandwidth parameter is more intuitive. In fact, the kernel bandwidth parameter regulates the level of detail with which the data space is analyzed; a large bandwidth means general analysis (few convergence locations), while a small bandwidth leads to a finer analysis (many convergence locations).

Here, we use the MS algorithm to the 4-dimensional space defined by the signal fea-

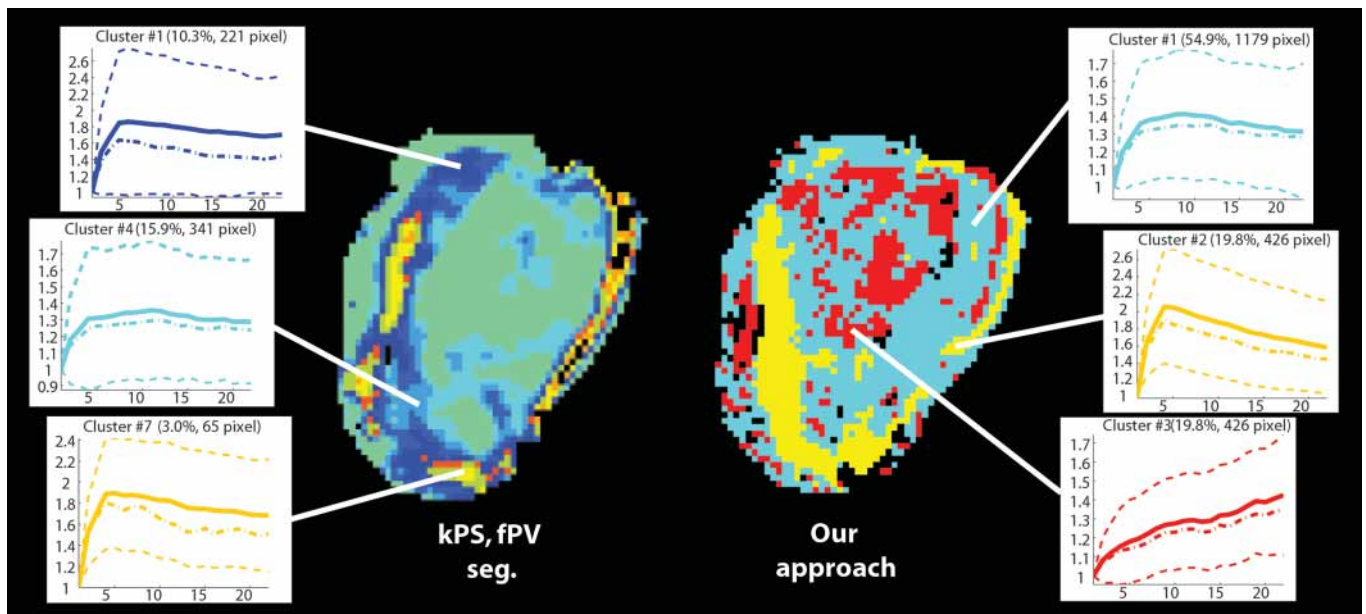


Fig. 3 Segmentation comparisons. On the left, the segmentation built on the kPS and fPV parameters; on the right, our segmentation. In the small boxes, we plot the mean signal (solid line), the median signal (dot-solid line), and the variance (dashed line) of the signal, respectively.

ture extraction. Since the bandwidth selection is crucial to find the correct segmentation (in the histological sense), we are supported by the medical researchers in this phase. Note that also subjects with the same tumor need different settings of the bandwidth. Therefore, we apply the MS clustering only to a subset of subjects with the same kind of tumor. Once the medical researchers have validated the clustering results, we use a classifier to distinguish the different kinds of tumoral tissues being more suitable to generalize the results [2].

3.3 SVM Classification

The involved classifier is the binary support vector machine (SVM) [9]. SVM constructs a maximal margin hyperplane in a high-dimensional feature space, by mapping the original features through a kernel function. Since the radial basis function (RBF) kernel has been used, two parameters C and γ needed to be estimated. According to suggestions reported in [15], data are normalized properly and parameters are estimated by combining grid search with leave-one-out cross-validation [2]. In order to extend the SVM to a multi-class framework, the one-against-all approach is carried out [2]. As

mentioned above, in our framework such learning-by-example approach is introduced to better generalize the results. In fact, the SVM is able to automatically detect the most discriminative characteristics of the detected clusters. Moreover, the training phase is intuitive and the testing (i.e., the classification) is faster than the clustering itself.

4. Results

The experiments performed in this paper are related to a series of investigations on the effects of a particular tumor treatment, using DCE-MRI techniques. Here, human mammary and pancreatic carcinoma fragments were subcutaneously injected in the right flank of 42 female rats at the level of the median-lateral. The details about the experiment outstand the scope of the paper (see [13] for details). After the injection of a contrast compound in the animals, MRI images were acquired for tumor localization and good visualization of extratumoral tissues.

4.1 Signal Feature Validation

As first experiment, we evaluate the effectiveness of the segmentation by comparing the

clusters obtained with the signal features with those obtained with the standard tumor microvessel parameters. In both cases we carefully tune the bandwidth, in order to find the best segmentation according with histological principles supported by medical researchers. ▶ Figure 3 shows one slice segmented with both approaches.

Even if apparently the segmentations seem visually similar, an accurate evaluation of the statistical properties of the obtained clusters reveals the better results obtained by the proposed approach. In Figure 3 the schemes show the mean curves of the DCE signals belonging to the same cluster. Beside the mean, for each cluster it is evidenced the median, and the variance. It is worth noting that 1) in general, good kPS - and fPV -based segmentations tend to be characterized by a large number of clusters. With a lower number of clusters, obtained by augmenting the MS bandwidth value, the segmentation decays in quality. In the figure, we report the three most meaningful clusters, out of nine; 2) the intra-cluster variance is, in general, high; 3) the mean curves of the clusters do not appear so different among each other as expected. After our clustering process instead, 1) the clusters are less in number and meaningful; 2) the intra-class variance is lower, as compared to the other clustering approach; 3) the profiles

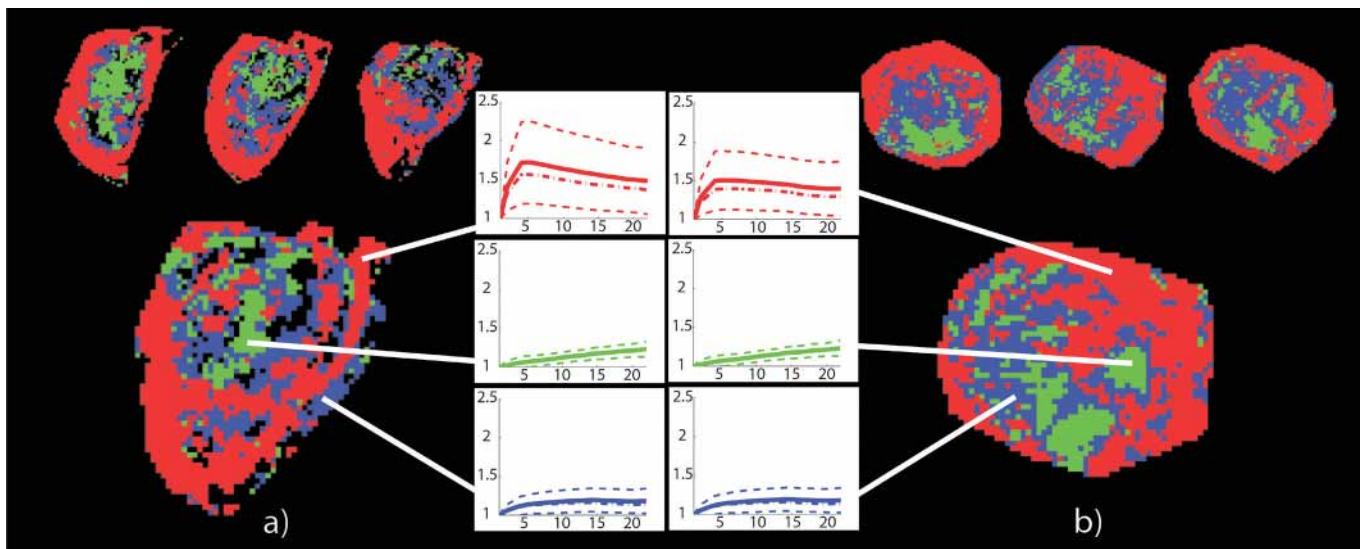


Fig. 4 Experiment 1: Clustering results obtained with the mean shift algorithm (a) and the SVM classifier (b) respectively. The curves of the mean-signals are also visualized for all the clusters.

of the mean curves are coherent with the expected behavior of the signals (in a histological sense). More in details, in the necrotic poorly vascularized (i.e., cluster 3) the contrast agent concentration enhances linearly. On the contrary, the active area (i.e., cluster 2) evidences a more rapid enhancement. The peak of the curve is reached in the early side of the signal and then it decays slowly. Finally, DCE signals of the area associated to cluster 1

show a rapid enhancement with a slow decay, meaning that zones of tissue previously vascularized are approaching a necrotic state.

4.2 Pipeline Validation

Following the proposed pipeline, we complete the experiment by segmenting a further subject (beside the subject used for signal fea-

ture validation) affected with the same kind of tumor of the previous cases. As mentioned before, different parameters are used to estimate the best clustering results in both the subjects. Therefore, the SVM is trained to recognize the three extracted classes. Indeed, the tissue classification is performed to a third unseen subject with the same tumor. ▶ Figure 4 shows four slices of both the segmentation obtained from the training and the

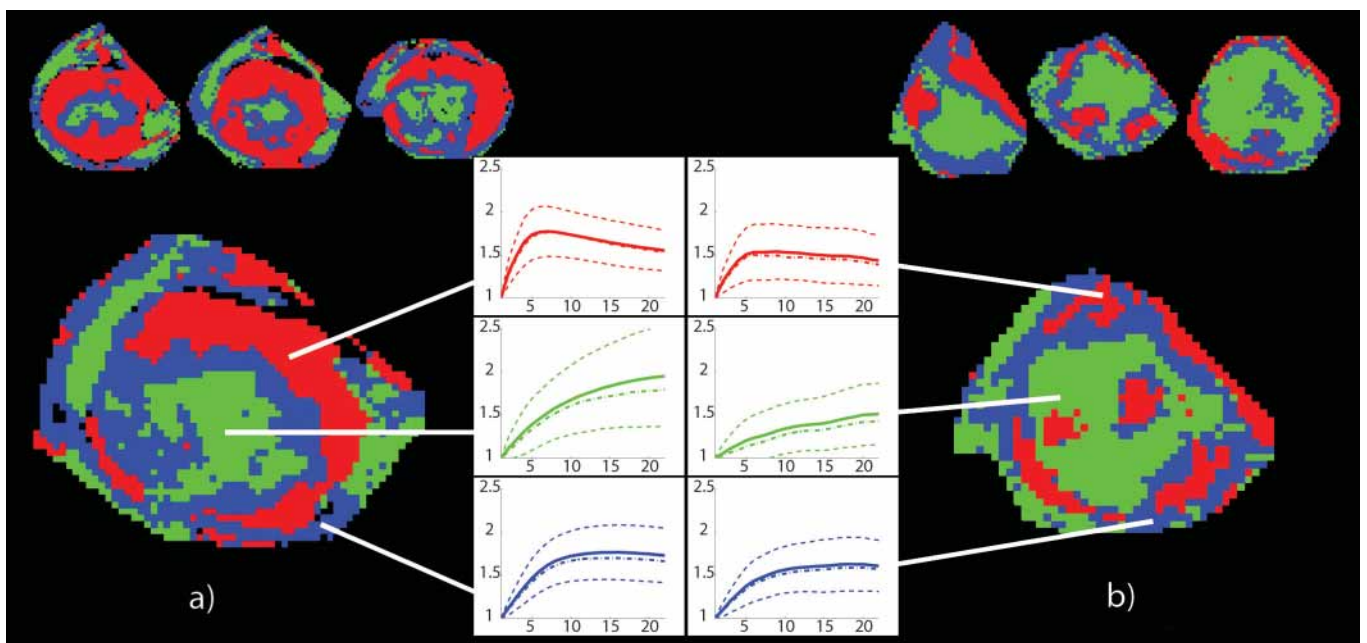


Fig. 5 Experiment 2: Clustering results obtained with the mean shift algorithm (a) and the SVM classifier (b) respectively. The curves of the mean-signals are also visualized for all the clusters.

testing subjects respectively. Moreover, it is also shown the respective statistics collected on each cluster provided by the classifier. Note that the extracted regions and the respective statistics in both the cases a and b in Figure 4 exhibit the same behavior.

The classification has been validated in two ways. The first one is based on the medical researcher analysis which confirmed the observations described above. As second validation, we applied the MS clustering also to the third subject, again by carefully tuning the parameters. By using the new obtained clustering results as ground truth, the SVM-based voxel classification reached the 89% of accuracy.

The same proposed pipeline is applied to three subjects with a new kind of tumor. Again, subjects 1 and 2 are used to train the SVM, while subject 3 represents the test. ▶ Figure 5 shows the clustering results and the related statistics. Also in this case the behavior of the SVM classifier is coherent with the clustering results and in accordance with the expectations of the medical researchers.

Note that in both the experiments, the estimated tumoral regions correspond to the one segmented by hand at steps 4 and 5 of the classical DCE-MRI analysis discussed in Section 2. We have carried out further experiments on new subjects affected by different kinds of tumors by observing mainly the same behavior: stable clusters of meaningful regions, as expected by the medical researchers.

5. Conclusions

In this paper, we introduce a new methodology, aimed at improving the analysis and the characterization of tumor tissues. The

multidimensional output obtained by non-invasive tissue analysis, namely the dynamic contrast-enhanced MRI (DCE-MRI) technique is considered. The signals of each voxel are parameterized by few and compact features which robustly summarize the shape of the signals, as expected by the medical researchers. We show that the proposed signal features perform better than standard tumor microvessel parameters, in segmenting the data. Moreover, we show the effectiveness of the proposed method based on the combination of clustering and classification techniques. The obtained results allow the evidencing of a histologically meaningful partition, that individuates tissue zones differently involved with the development of the tumor. The proposed method achieves two goals: 1) it permits an analysis of the tissue more precise and 2) faster than the manual analysis classically performed. These two results assess that the proposed machine learning approach well behaves with medical segmentation and classification issues, related to the DCE-MRI context.

References

1. Lau PY, Ozawa S, Voon FCT. Using Block-based Multiparameter Representation to Detect Tumor Features on T2-weighted Brain MRI Images. *Methods Inf Med* 2007; 46: 236–241.
2. Duda RO, Hart PE, Stork DG. *Pattern Classification*. John Wiley and Sons, second edition; 2001.
3. Castellani U, Cristani M, Combi C, Murino V, Sbarbati A, Marzola P. Visual MRI: Merging information visualization and non-parametric clustering techniques for MRI dataset analysis. *Artificial Intelligence in Medicine* 2008; 44 (3): 171–282.
4. Buckley DL. Uncertainty in the analysis of tracer kinetics using dynamic contrast enhanced T1-weighted MRI. *Magnetic Resonance Med* 2002; 47: 601–606.
5. Harrer JU, Parker GJ, Haroon HA, Buckley DL, Embelton K, Roberts C, et al. Comparative study of methods for determining vascular permeability and blood volume in human gliomas. *Magnetic Resonance Imaging* 2004; 20: 748–757.
6. Lavinia C, De Jongea MC, Van de Sandeb MGH, Takb PP, Nederveena AJ, Maas M. Pixel-by-pixel analysis of DCE MRI curve patterns and an illustration of its application to the imaging of the musculoskeletal system. *Magnetic Resonance Imaging* 2007; 25: 604–612.
7. Tofts PS, Briks G, Buckley DL, Evelhoch JL, Henderson E, Knopp MV et al. Estimating kinetic parameters from dynamic contrast enhanced T1-w MRI of a diffusible tracer: standardized quantities and symbols. *Magnetic Resonance Imaging* 1999; 10: 223–232.
8. Comaniciu D, Meer P. Mean shift: A robust approach toward feature space analysis. *IEEE Trans Pattern Anal Mach Intell* 2002; 24: 603–619.
9. Burges C. A tutorial on support vector machine for pattern recognition. *Data Mining and Knowledge Discovery* 1998; 2: 121–167.
10. Stoutjesdijk MJ, Veltman J, Huisman MD, Karssemeijer N, Barents, J et al. Automatic analysis of contrast enhancement in breast MRI lesions using mean shift clustering for ROI selection. *Journal of Magnetic Resonance Imaging* 2007; 26: 606–614.
11. Twellmann T, Saalbach A, Muller C, Nattkemper TW, Wismuller A. Detection of suspicious lesions in dynamic contrast-enhanced MRI data. *Engineering in Medicine and Biology Society* 2004. pp 454–457.
12. Leistriz L, Hesse W, Wustenberg T, Fitzek C, Reichenbach JR, Witte H. Time-variant analysis of fast-fMRI and dynamic contrast agent MRI sequences as examples of 4-dimensional image analysis. *Methods Inf Med* 2006; 45: 643–650.
13. Marzola P, Ramponi S, Nicolato E, Lovati E, Sandri M, Calderan L, Crescimanno C, Merigo F, Sbarbati A, Grotti A, Vultaggio S, Cavagna F, Lo Russo V, Osculati F. Effect of tamoxifen in an experimental model of breast tumor studied by dynamic contrast-enhanced magnetic resonance imaging and different contrast agents. *Investigative radiology* 2005; 40: 421–429.
14. Marzola P, Degrassi A, Calderan L, Farace P, Crescimanno C, Nicolato E, Giusti A, Pesenti E, Terron A, Sbarbati A, Abrams T, Murray L, Osculati F. In vivo assessment of antiangiogenic activity of su6668 in an experimental colon carcinoma model. *Clin Cancer Res* 2004; 2: 739–50.
15. Chang CC, Lin CJ. LIBSVM: a library for support vector machines. 2001.